Michelson interferometer null may confirm transverse Doppler Effect

Robert A. Woodruff
Center for Astrophysics and Space Astronomy, Astrophysics Research Laboratory, University of Colorado, 593 UCB, Boulder, Colorado 80309-0593, USA.
raw@colorado.edu

(Received 12-17-2013; published xx-xx-xxxx)

ABSTRACT

We analyze fringe formation within Michelson-like experiments as viewed by relativistic inertial observers. Our analysis differs from previous work because we include optical misalignment of the beamsplitter of the interferometer due to the anamorphic geometry of relativistic Lorentz contraction. We conclude that inertial frame equivalence of Michelson-like experiments provide verification of the transverse Doppler Effect and exclude any model incorporating the relativistic Lorentz contraction effect.

PACS: 03.30.+p, 95.75.Kk, 42.90.+m, 11.30.Cp

1. INTRODUCTION

In the 1880's Michelson and Morley [1] performed experiments in search of a propagation medium believed at the time essential for light propagation as a wave phenomenon. The experiments used Michelson interferometers designed and configured to detect the effect of the proposed fixed ether. The surprising null results led to additional experiments by several observers using variations of Michelson interferometer configurations and eventually to the rejection of the ether concept. The special theory of relativity [2] explained the null results by assuming two postulates and derived the concepts of Lorentz contraction and time dilation. The two postulates, the 1st postulate of inertial frame equivalence and the 2nd postulate of source-referred constancy of the speed of light, yielded a model that fully predicted the null results of the Earth-based experiments and via the 1st postulate predicted that the null will hold for any inertial observer in uniform motion relative to the interferometer.

However, Lorentz contraction within special relativity (SR) is spatially asymmetric contracting only in the direction of motion. This asymmetry would optically misalign any optical component within the interferometer that is not initially parallel to or perpendicular to the direction of relative motion. The SR model does not account for this optical misalignment. This paper corrects this omission by incorporating the asymmetric spatial effects of Lorentz contraction on optical alignment of interferometer components, specifically alignment change of its beamsplitter. We find that if the special relativistic model were to include beamsplitter tilt due to Lorentz contraction, it would fail to predict the null result of the experiment for inertial observers moving much faster than the annual orbital velocity of the Earth. Therefore, SR apparently provides only an approximate description of relativity physics since it fails to meet the standards of Einstein's 1st postulate that physical effects should be independent of relative motion of the observer.

2. FRINGE FORMATION IN MICHELSON INTERFEROMETER

A. Geometry

A Michelson interferometer, in its unprimed K rest frame shown in Figure 1 and in the primed K' frame of a moving observer shown in Figure 2, can be aligned to form a null interference fringe if its arms are of equal lengths in its rest frame. (The beamsplitter thickness and its accompanying refractive compensator plate are omitted. This will not affect the conclusions of this paper.) An incoming collimated plane wavefront, incident from the left parallel to the arm that transmits through the beamsplitter, reaches the beamsplitter (S). The beamsplitter divides its complex amplitude into two beams: one beam that transmits undeviated through S to mirror M1 and the second beam that reflects from S to mirror M2. The first beam, referred to here-in as Path 1, passes horizontally to mirror M1which reflects it back to S. The beamsplitter then reflects this returned beam downward in the figure to the image plane. The second beam, Path 2, reflects from the beamsplitter to mirror M2 that, in turn, reflects it back to the beamsplitter. It then transmits undeviated through the beamsplitter to the same image plane. The complex amplitudes of the wavefronts of the two divided beams add coherently in the space of the image plane forming optical interference fringes.

B. Model of Michelson interferometer fringes

To determine conditions for null fringe formation, we derive the total elapsed times, as observed by each observer from the instant at time $t = t' = 0$ that the center light ray encounters the beamsplitter to instant it reaches the image plane, encountered by the wavefronts in their respective arms of the interferometer.

The optical path length and other variables including physical length and time for light propagating initially horizontally from S to M1 back to S and then vertically to the image plane is designated by the index $i = 1$. We designate these variables for light propagating solely in the vertical arms of the interferometer with the index $i = 2$.

Figures 1 and 2 define the model variables viewed by each observer. Table 1 summarizes them. The variable t refers to the elapsed time for the light beam to transit the respective light path labeled with notation and indices t_i, t_{ij}, t_i', and t_{ij}', where $i = 1,2$ as defined previously and $j = 1,2,3$ which refers to the three arms of the interferometer, respectively. The index $j = 1$ refers to propagation from the beamsplitter to the mirror, $j = 2$ to propagation from the mirror to the beamsplitter, and $j = 3$ for propagation from the beamsplitter to the image.

Reference Figures 1 & 2	Moving observer frame: K′	Rest frame: K
Distance Beamsplitter to Mirror M1	l_1'	l_1
Distance Beamsplitter to Mirror M2	l_2'	l_2
Distance Beamsplitter to image plane	l_3'	l_3
Elapsed time interval	t_i', t_{ij}'	t_i, t_{ij}

Table 1: Model variables

When $i = 1$, the total time delay observed in frame K is $t_1 = t_{11} + t_{12} + t_{13}$: the sum of propagation temporal interval for $j = 1$ from S to M1, t_{11}; plus the time interval for $j = 2$ to propagate from M1 back to S, t_{12}; plus time interval for $j = 3$ to propagate from S to image plane, t_{13}. When $i = 2$, the total elapsed time delay observed in frame K is $t_2 = t_{21} + t_{22} + t_{23}$: the sum of light propagation time from S to M2 ($j = 1$), t_{21}; plus time to propagate from M2 back to S ($j = 2$), t_{22}; plus the propagation time from S to

image plane ($j = 3$), t_{23}. Using identical notation and logic the path through mirror M1 in frame K′ is $t_1' = t_{11}' + t_{12}' + t_{13}'$ and that of the path through mirror M2 in frame K′ is $t_2' = t_{21}' + t_{22}' + t_{23}'$.

We designate the incident wavelength by λ in the rest frame and λ' in the moving frame. We assume the wavelength is unchanged for a given observer in interferometer arms that lie parallel to the incident beam, that is, along the horizontal path, because no physical effect occurs that could change the incident wavelength. Along the vertical path, by definition the rest frame observer will sense the rest frame wavelength λ . In the vertical direction light propagation as viewed by the horizontally moving observer, we allow the wavelength to change to λ_{Vert}' . We designate the speed of light as c in the rest frame. In the moving observer frame, we assume speed of light also to be a constant c , unless otherwise indicated.

Referring to Figure 1 for $i = 2$, the propagation time intervals viewed by the rest frame observer in the arms from beamsplitter (S) to Mirror (M2) to S to image plane (I) are

$$t_{21} = t_{22} = \frac{l_2}{c} \text{ and } t_{23} = \frac{l_3}{c}. \quad (1)$$

Since Snell's law requires the angle of incidence at mirror M2 to equal the angle of reflection, the geometry of Figure 2 shows the optical path length l_2' from the beamsplitter to mirror M2 equals the optical path length to the beamsplitter after reflection from mirror M2. Therefore referring to Figure 2 for the moving frame,

$$t_{21}' == \frac{l_2'}{c},\ t_{22}' = \frac{l_2'}{c} \text{ and } t_{23}' = \frac{l_3'}{c}. \quad (2)$$

Similarly for $i = 1$, in the arms from the beamsplitter (S) to Mirror (M1) to S to image plane (I).

$$t_{11} = t_{12} = \frac{l_1}{c} \text{ and } t_{13} = \frac{l_3}{c}. \quad (3)$$

$$t_{11}' = \frac{l_1'}{(c - v)}, t_{12}' = \frac{l_1'}{(c + v)}, \text{ and } t_{13}' = \frac{l_3'}{c}. \quad (4)$$

The total optical path length in wavelengths of light is [3, p.48]

$$N_i = \sum_j \frac{c_j t_{ij}}{\lambda_j} \text{ with } i = 1,2 \text{ and } j = 1,2,3. \quad (5)$$

Also, $$N_i' = \sum_j \frac{c_j' t_{ij}'}{\lambda_j'} \text{ with } i = 1,2 \text{ and } j = 1,2,3. \quad (6)$$

Evaluating Equations (5) and (6) using Equations (1), (2), and (3), we find

$$N_1 = \frac{2l_1}{\lambda} + \frac{l_3}{\lambda} \quad (7a)$$

$$N_2 = \frac{2l_2}{\lambda} + \frac{l_3}{\lambda} \quad (7b)$$

and $$N_2' = \frac{2l_2'}{\lambda_{Vert}'} + \frac{l_3'}{\lambda_{Vert}'}. \quad (7c)$$

Evaluating Equation (6) using Equation (4), we find

$$N_1' = \frac{ct_{11}'}{\lambda'} + \frac{ct_{12}'}{\lambda'} + \frac{l_3'}{\lambda_{Vert}'} = \frac{2l_1'\gamma^2}{\lambda'} + \frac{l_3'}{\lambda_{Vert}'} \quad (8)$$

where $\gamma = 1/\sqrt{(1-\beta^2)}$ and $\beta = \frac{v}{c}$. (9)

As shown in Figure 2, the angle σ from the vertical axis to the center ray in the moving observer frame is given by

$$\sigma = \arcsin(\beta). \quad (10)$$

By the geometry in Figure 2,

$$l_2' = \frac{l_2}{\cos(\sigma)} = \gamma l_2 \quad (11)$$

By the same reasoning yielding Equation (11)

$$l_3' = \gamma l_3. \quad (12)$$

For use latter in this paper, we note that the wavelength due to the transverse Doppler Effect measured at an angle $\frac{\pi}{2} - \sigma$ from the direction of a moving source with incident wavelength λ' is

$$\lambda_T(\sigma) = \gamma\lambda'[1 - \beta\cos(\frac{\pi}{2} - \sigma)]. \text{ [3, p144]} \quad (13)$$

Per Equation (10), $\sin(\sigma) = \beta$, so the transverse Doppler wavelength along l_2' becomes

$$\lambda_T(\sigma) = \gamma\lambda'[1 - \beta^2] = \frac{\lambda'}{\gamma} \quad (14)$$

If the arm lengths are equal in the rest frame, $l_1 = l_2$, applying Equations (7a) and (7b) trivially yields $\Delta N = N_2 - N_1 = 0$, so a null fringe forms. Einstein's first postulate [2] requires inertial frame equivalence. Therefore,

$$\Delta N' = N_2' - N_1' = 0. \quad (15)$$

C. Conditions that maintain null fringe

We consider three sets of assumptions that may satisfy Equation (15) and refer to these as Hypothesis A, B, and C, respectively.

Under Hypothesis A and B, the speed of light is a constant for all observers. Applying Equations (7c) and (8), the general expression

$$\lambda' l_2 = \gamma\lambda_{Vert}' l_1' \quad (16)$$

follows from the null fringe condition expressed in Equation (15).

Hypothesis A then assumes no Lorentz contraction occurs. Thus, $l_1' = l_1 = l_2$. Setting the incident wavelength to λ' and the vertical path wavelength to λ_{Vert}, Equation (16) implies $\lambda_{Vert}' = \frac{\lambda'}{\gamma} = \lambda_T$, precisely the transverse Doppler wavelength given in Equation (14). Therefore, inertial frame equivalence applied to Michelson's experimental fringe null result may confirm the Doppler Effect at transverse angles, but only if Lorentz contraction does not occur.

Hypothesis B also assumes constant speed of light, but without the Doppler Effect. We set $\lambda'_{Vert} = \lambda'$ in Equation (16). If $l_1 = l_2$, Equation (16) implies that $l_1 = \gamma l'_1$. Therefore, Michelson's experimental fringe null result may confirm a spatial dimension contraction effect if length contraction does not modify the angular alignment of the optical components within the interferometer.

A third case, Hypothesis C, assumes observer-dependent speed of light and no Doppler Effect. If $c'_{11} = c + v$, $c'_{12} = c - v$ and c is the speed of light in the vertical paths, using Equation (6) one can easily derive

$$N'_2 = \frac{2l'_2}{\lambda'} + \frac{l'_3}{\lambda'} \text{ and } N'_1 = \frac{l'_1(c+v)}{c\lambda'} + \frac{l'_1(c-v)}{c\lambda'} + \frac{l'_3}{\lambda'} = \frac{2l'_1}{\lambda'} + \frac{l'_3}{\lambda'}. \quad (17)$$

Applying Equation (15) using Equations (11) and (17) and $l_1 = l_2$, then yields $l'_1 = \gamma l_1$. Therefore, Michelson's experimental fringe null result may also confirm a spatial contraction effect, if such effect does not modify the angular alignment of the optical components of the interferometer, but in this case with observer velocity dependent speed of light.

D. Anamorphic distortion of Lorentz contraction tilts the beamsplitter

Within special relativity, Lorentz contraction introduces an asymmetric transformation of the spatial dimensions of a moving object. These distortions manifest in two distinct geometric changes. When viewed by a moving observer, a one-dimensional ruler moving parallel to its length would appear shortened and a one-dimensional ruler moving perpendicular to its length would be unchanged in length. Special relativity incorporates these changes and rigorously explains the experimental null result for all inertial observers. However, another effect would occur due to Lorentz contraction that has not been included in such analyses until this paper.

Figure 3 illustrates the effect with the relative velocity shown parallel to the x-axis. Consider two points lying on the front reflective surface of the beamsplitter: one the point where the center incident ray intersects the surface $(0,0)$ and another at arbitrary coordinate (x, y). In this example, we assume a 45 degree angle of incidence at the beamsplitter, θ, in the rest frame of the interferometer to match Michelson's 1881 and 1887 experimental geometry. Viewed in the moving observers frame, the x-coordinate of the offset point relative to the center point changes, but the associated y-coordinate is unchanged. Therefore, the beamsplitter will tilt viewed in the moving frame.

The offset surface coordinate transforms to $(x, y) = (\frac{y}{\gamma}, y)$, [3, p. 97] so the angle of incidence becomes $\theta = \arctan\left[\frac{1}{\gamma}\right]$ in the moving frame. The center ray of the wavefront reflected from this surface will be deviated by $\delta = 2\Delta\theta$ from the vertical y-axis, where $\Delta\theta = \frac{\pi}{4} - \theta$. Straightforward algebra yields $\delta = 2\arctan\left[\frac{(\gamma-1)}{(\gamma+1)}\right]$.

The angle from the incident ray to the reflected ray then becomes $\frac{\pi}{2}-\Delta=\frac{\pi}{2}-\sigma+\delta$ where σ is defined in Equation (10). Combining this effect with that shown in Figure 2, angle σ in Equation (11) would be replaced with the angle

$$\Delta=\sigma-\delta \tag{18}$$

By geometry of Figure 2, the vertical optical path length becomes $l_2'=\frac{l_2}{\cos(\Delta)}$. Combining Equations (15), (7c) and (8), applying Lorentz contraction in the horizontal arm, $l_1'=\frac{l_1}{\gamma}$ and applying $\Delta N=N_2-N_1=0$ with $l_1=l_2$, we find

$$\gamma=\frac{\lambda'}{\lambda'_{Vert}\cos(\Delta)}. \tag{19}$$

If $\lambda'_{Vert}=\lambda'$, the change in path length due to beamsplitter tilt will prevent a null fringe unless

$$\gamma=\frac{1}{\cos(\Delta)}. \tag{20}$$

The angle Δ varies as a function of β from zero to a maximum value of approximately 25.6 degrees near $\beta\approx 0.74$. Equation (20) only holds if $\beta<<1$. Therefore, any solution incorporating Lorentz contraction without including the beamsplitter tilt changes fails to extend Michelson-like experimental results to all inertial observers.

The model incorporating the assumptions of Hypothesis A fully predicts the measured null of the Michelson-like experiments for all inertial observers. Hypothesis A evidently confirms the transverse Doppler Effect (TDE).

3. DISCUSSION

Thim [4] points out that TDE is "one of few direct consequences of special relativity as its follows directly from time dilation", thereby establishing the theoretical importance of confirmation of the TDE. Olin [5] notes that TDE is difficult to measure directly since a small error in angle would confuse the second order effect by the first order effect. However, it has been rigorously verified by using relativistic ion beams. (See Ives [6], Kaivola [7], Kholmetskii [8], Olin [5], and others). Woodruff [9] proposed an optical mechanism for aberration of starlight, as opposed to the special relativistic mechanism, and proposed an optical measurement that could provide an independent test of time dilation because the special relativistic mechanism requires time dilation.

Robertson [10] systematically develops logic that shows that three experiments, those by Michelson [1], Kennedy [11], and Ives [6]; taken together, observationally establish SR. He shows that SR effects must simultaneously include both Lorentz contraction and time dilation. Einstein [2] postulated this symmetry based on group theory. These three experiments observationally confirm this combination [10]. Theoretically and observationally one cannot have one without the other.

However, our paper shows that optical misalignment due to Lorentz contraction will occur. This effect is not included in published models of the interferometric experiments. Thus, we question the basis for the conclusion that SR explains the interferometric experiments.

Our results also suggest that Michelson-like experimental results provide optical interferometric verification of TDE and hence of time dilation.

4. CONCLUSION

We include the effects of Lorentz contraction on optical alignment of Michelson interferometers as viewed by inertial observers. Recognizing that Lorentz contraction is spatially asymmetric, we model the resultant beamsplitter tilt and conclude that this observer velocity dependent effect eliminates any model that includes length contraction, except perhaps as an approximate description holding only at relatively small velocities where the tilt error is small enough to not affect the measured result. TDE without Lorentz contraction yields a model that fully explains the measured null result for all inertial observers.

Acknowledgements

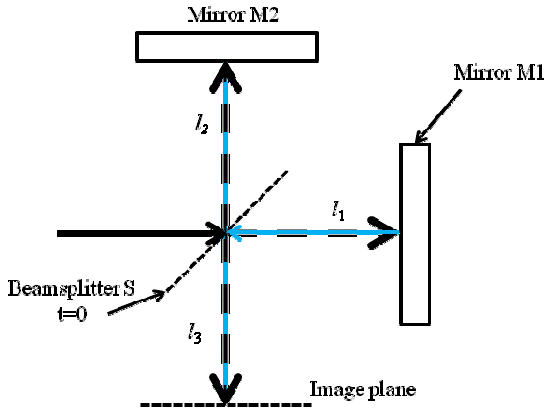


Figure 1: Interferometer viewed by observer fixed to Frame K

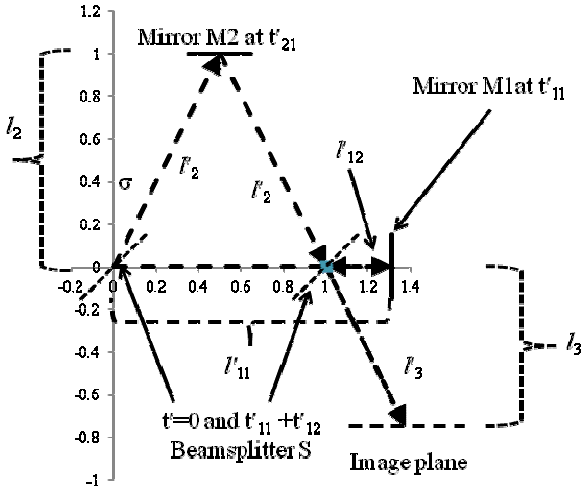


Figure 2: Interferometer viewed in moving observer's Frame K′, if optical misalignments due to beamsplitter tilt caused by Lorentz contraction do not occur. Note: l'_1 is axial distance from S to M1 at time t′=0.

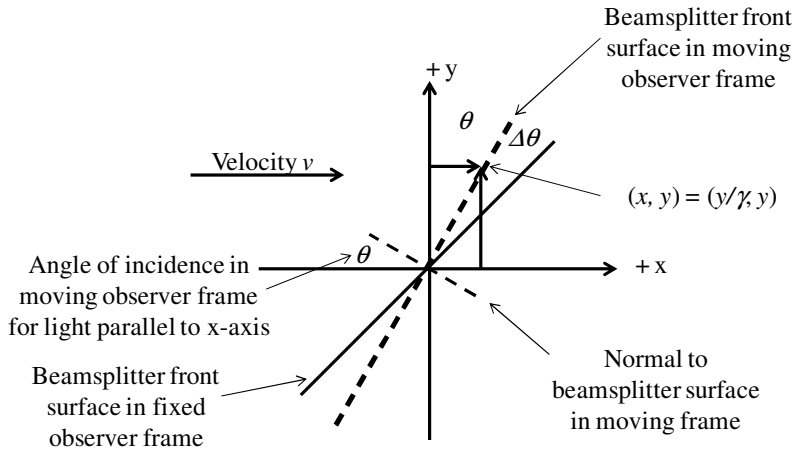


Figure 3: Beamsplitter tilt due to Lorentz contraction

References

[1] A. A. Michelson, "The relative motion of the Earth and the luminiferous ether," Am. J. Sci. 22, 120–129 (1881). & A. A. Michelson and E. W. Morley, "On the relative motion of the Earth and the luminiferous ether," Am. J. Sci. 34, 333–345 (1887).
[2] A. Einstein "On the Electrodynamics of Moving Bodies", Annalen der Physik, **17**, (1905) 891.
[3] A.P. French, "Special relativity", (W.W. Norton & Company Inc., New York) 1968, pp. 48, 144, and 97 and 144.
[4] Thim, H.W., "Absence of the relativistic transverse Doppler shift at microwave frequencies," Instrumentation and Measurement, IEEE Transactions on , vol.52, no.5, pp.1660,1664, Oct. 2003
[5] A. Olin, T.K. Alexander, O. Hausser, A.B. McDonald, "Measurement of the Relativistic Doppler Effect Using 8.6-MeV Capture γ Rays", Phys. Rev. D 8, 1633–1639 (1973).
[6] H.E. Ives, G.R. Stilwell, J. Opt. Soc. Am. **28**, 215 (1938); J. Opt. Soc. Am. **31**, 369 (1941).
[7] M. Kaivola, O. Poulsen, E. Riis, S.A. Lee, Phys. Rev. Lett. **54**, 255 (1985).
[8] A L Kholmetskii et al, "Kündig's experiment on the transverse Doppler shift re-analyzed", Phys. Scr. **77** (2008).
[9] R. A. Woodruff. "Optical mechanism for aberration of starlight", **29**, No. 7, J. Opt Soc. Am. A, p.1217, (July 2012).
[10] H. P. Robertson, H. P. (1949). "Postulate versus Observation in the Special Theory of Relativity". Reviews of Modern Physics **21** (3): 378–382, (1949).
[11] R. J. Kennedy and E. M. Thorndike, "Experimental Establishment of the Relativity of Time". Phys. Rev. 42, 400, (1932).